Appl. Phys. B 42, 215–219 (1987)

Applied Physics B Photophysics and Laser Chemistry

Four-Wave Mixing Reflectivity of Silicon at 1.06 μm: Influence of Free-Carrier Absorption

H.-J. Eichler, Jun Chen, and K. Richter

Optisches Institut, Technische Universität, Straße des 17. Juni 135, D-1000 Berlin 12

Received 27 October 1986/Accepted 22 December 1986

Abstract. The phase-conjugate reflectivity obtainable by degenerate four-wave mixing in silicon at a 1.06 μm is calculated including free-carrier absorption. A maximum reflectivity of more than 100% is possible. The dependence of the reflectivity on the signal and pump energy densities up to 70 mJ/cm^2 is measured and found to agree with theory. The wave-front-correction property of DFWM is demonstrated with a lens in the signal beam.

PACS: 42.65.Gv

Four-wave mixing (FWM) has been studied extensively in recent years, because it allows wave-front-correction by phase conjugation. The first experiments of degenerate four-wave mixing (DFWM) with a 1.06 μm Nd:YAG-laser in silicon have been reported by Woerdman and Bolger [1, 2], and by Jarasiunas and Vaitkus [3] for real-time holography. Because the band-gap of silicon at room temperature ($\sim$1.1 eV) is matched to the photon energy of the Nd:YAG-laser, free carriers are produced by absorption. The corresponding refractive index change leads to efficient DFWM.

More experiments of DFWM in silicon have been performed by Jain and Klein [4–6]. They have measured the diffraction efficiency of free-carrier gratings, the reflectivity of DFWM, and the third-order susceptibility.

In this paper we report calculations of the reflectivity of DFWM at 1.06 μm in silicon including free-carrier absorption. The signal beam and one of the pump beams produce a spatially periodic electron-hole density which change the refractive index n and the absorption coefficient α [7, 8]. The other pump beam which propagates opposite to the first one, is diffracted by the light-induced grating. The first-order diffracted beam is phase conjugated with respect to the signal beam. The DFWM reflectivity saturates due to nonlinear absorption at higher energy densities. The calculations are compared with measurements.

1. Experimental Arrangement

The experimental arrangement is shown schematically in Fig. 1. A Q-switched Nd:YAG-laser with an amplifier emitted a laser pulse with the duration of $\tau_i \approx 15$ ns, the total pulse energy was 30 mJ. The coherence length was approximately 1 cm. Therefore we used an optical delay to adjust the path difference between the signal E_s and pump beam E_{p1}. The angle between E_s and E_{p1} was kept at 1°. The beam splitter BS_2 and mirrors M_2 and M_3 generated the two counter propagating pump beams E_{p1} and E_{p2} with nearly the same intensity. High-purity silicon, weakly

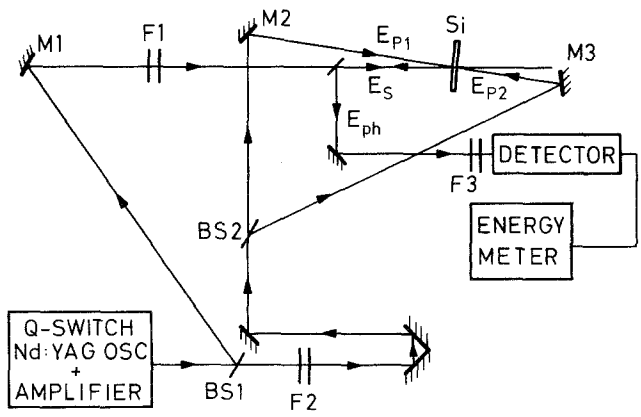

Fig. 1. Experimental arrangement for four-wave mixing in silicon

p-doped, cut normal to the ⟨1, 0, 0⟩ axis, was used. The surfaces of the sample were polished and coated with SiO, so that the reflectivity at 1.06 μm was smaller than 2% and the sample could be inserted perpendicular to the pump beam. The silicon crystal together with the two antiparallel pump beams formed a phase conjugating mirror (PCM). The energy of the beam reflected by the PCM was measured with an energy meter (Rj-7100).

2. Theory of Phase-Conjugation in Silicon

2.1. Dependence of Carrier Density and Refractive Index on Incident Laser-Beam Energy Density

An incident light wave with intensity $I(y, t)$, energy density $E(y, t)=\int I(y, t)dt$ and photon density $Q=E/h\nu$ is absorbed in the silicon sample and produces a carrier distribution given by [9]:

$$N(y, x, t)=\frac{\alpha Q(y, t)\exp(-\alpha x)}{1+(\sigma/2)Q(y, t)\,[1-\exp(-\alpha x)]}. \tag{1}$$

Here x is the distance from the crystal surface, α the linear absorption coefficient, σ the free-carrier absorption cross-section and y a coordinate perpendicular to the propagation direction of the light wave.

The average carrier density in the x-direction is obtained as

$$N(y, t)=\frac{1}{d}\int_0^d N(y, x, t)dx$$

$$=\frac{2}{\sigma d}\ln\left\{1+\frac{\sigma}{2}Q(y, t)\,[1-\exp(-\alpha d)]\right\}, \tag{2}$$

where d is the sample thickness. Note that $N(y, t)$ depends only on the incident energy density $Q(y, t)$ and not on the direction of incidence. Equation (2) will be used therefore in the following to approximate the average carrier density also for antiparallel excitation beams.

In a four-wave mixing experiment, the incident photon density is given by the two antiparallel pump beams Q_{p1}, Q_{p2} and the signal beam Q_s

$$Q(y, t)=Q_{p1}+2\sqrt{Q_{p1}Q_S}\cos qy+Q_s+Q_{p2} \tag{3}$$

with $q=2\pi/\Lambda$ being the grating constant. Only interference of Q_{P1} and Q_s is considered. Interference of Q_{P1} and Q_s with Q_{P2} produces a grating with periods of the order of $\lambda/2n$. Free-carrier gratings with such small periods decay rapidly and are not considered therefore.

Combination of (2) and (3) gives the spatially modulated carrier density. Assuming that $2\sqrt{Q_sQ_{p1}}\ll Q_{p1}+Q_{p2}+Q_s$, the spatial amplitude $\Delta N(y, t)$ of the carrier density is calculated as

$$\Delta N(t)=\frac{\partial N(y, t)}{\partial Q}\,2\sqrt{Q_{p1}Q_s}$$

$$=\frac{[1-\exp(-\alpha d)]\,2\sqrt{Q_{p1}Q_s}}{d\{1+(\sigma/2)\,(Q_{p1}+Q_{p2}+Q_s)\,[1-\exp(-\alpha d)]\}}. \tag{4}$$

The spatially modulated carrier density produces a refractive index modulation with amplitude

$$\Delta n(t)=n_{eh}\Delta N(t). \tag{5}$$

Here n_{eh} is the "dispersion volume", i.e. the refractive index change due to one electron-hole pair per unit volume.

The free-carriers also decrease the sample transmission according to

$$T=\exp[-\alpha d-\sigma N(t)d]. \tag{6}$$

The average carrier density $N(t)$ is determined by (2) and (3) with $\cos qy=0$ resulting in

$$T=\frac{\exp(-\alpha d)}{\left\{1+\frac{\sigma}{2}(Q_{p1}+Q_{p2}+Q_s)\,[1-\exp(-\alpha d)]\right\}^2}. \tag{7}$$

2.2. Four-Wave Mixing Reflectivity

The reflected, phase-conjugated wave is produced by diffraction of the backward pump wave with intensity $I_r(t)$ and corresponding energy and photon densities. Using the Bessel-function approximation [8, 10] for a thin phase grating one obtains

$$I_r(t)=TI_{p2}(t)\,J_1^2\left(\frac{2\pi\Delta n(t)d}{\lambda}\right). \tag{8}$$

If the signal energy density and therefore Δn are sufficiently small, a first-order expansion of the Bessel function J_1 yields

$$I_r(t)=\left(\frac{\pi\Delta n(t)d}{\lambda}\right)^2 TI_{p2}(t). \tag{9}$$

This approximation is valid also for a thick phase grating. Introducing (4, 5, 7) gives

$$I_r(t)=\frac{(2\pi n_{eh}/\lambda)^2[1-\exp(-\alpha d)]^2\exp(-\alpha d)Q_{p1}(t)Q_s(t)I_{p2}(t)}{\left\{1+\frac{\sigma}{2}(Q_{p1}+Q_s+Q_{p2})\,[1-\exp(-\alpha d)]\right\}^4}. \tag{10}$$

For further evaluation it is assumed that the temporal pulse shapes of the three incident waves

$I_{p1}(t)$, $I_{p2}(t)$, $I_s(t)$ are the same. We therefore introduce

$$Q(t)=\frac{1}{h\nu}\int I dt=\frac{1}{2}[Q_{p1}(t)+Q_{p2}(t)+Q_s(t)] \tag{11}$$

and

$$\begin{aligned} Q_{p1}(t)&=\frac{1}{h\nu}\int I_{p1}(t)dt=c_1Q(t)\,,\\ Q_{p2}(t)&=\frac{1}{h\nu}\int I_{p2}(t)dt=c_2Q(t)\,,\\ Q_s(t)&=\frac{1}{h\nu}\int I_s(t)dt=c_sQ(t)\,. \end{aligned} \tag{12}$$

The total reflected pulse photon density is obtained by integration of (10)

$$\begin{aligned} Q_r&=\frac{1}{h\nu}\int I_r(t)dt\\ &=(2\pi n_{eh}/\lambda)^2[1-\exp(-\alpha d)]^2\exp(-\alpha d)c_1c_2c_s\\ &\quad\times\int_0^Q\frac{Q^2(t)dQ(t)}{\{1+\sigma Q(t)\,[1-\exp(-\alpha d)]\}^4}\,. \end{aligned} \tag{13}$$

Here $Q=Q(t=\infty)$ is the total average pulse phonton density of the three incident beams.

Performing the integration in (13), the four-wave mixing reflectivity is obtained as

$$R=\frac{Q_r}{c_sQ}=R_{\max}\frac{27(Q/Q_{\max})^2}{(1+2Q/Q_{\max})^3}\,. \tag{14}$$

This equation describes a quadratic dependence of the reflectivity for small pulse energies Q and saturation at large Q due to free carrier absorption (Fig. 2),

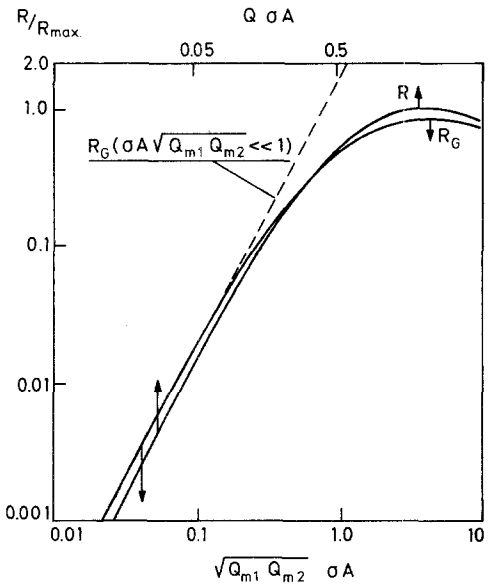

Fig. 2. Reflectivity of DFWM in silicon versus normalized pump energy $Q\sigma A$. $R-Q\sigma A$ is for plane waves, $R_G-\sqrt{Q_{m1}Q_{m2}}\,\sigma A$ is for Gaussian beams

The maximum reflectivity

$$R_{\max}=\left(\frac{4\pi n_{eh}}{9\lambda\sigma}\right)^2 c_1c_2\exp(-\alpha d) \tag{15}$$

is obtained at

$$Q_{\max}=\frac{2}{\sigma[1-\exp(\alpha d)]}\,. \tag{16}$$

According to (15) the largest reflectivities are expected for very thin samples ($d\ll 1/\alpha$). However, the necessary pump photon densities $Q_{\max}$ become very large in this case. For practical applications the pump energy density is limited by surface break-down to several 100 mJ/cm^2.

If free-carrier absorption is neglected, the optimum thickness is derived to

$$d_{\text{opt}}=(1/\alpha)\ln 3\approx 1/\alpha\,. \tag{17}$$

2.3. *Gaussian Average of* FWM *Reflectivity*

Four-wave mixing experiments are often performed with TEM_{00} laser beams. The photon density is given by

$$Q=Q_m\exp(-2r^2/w^2)\,. \tag{19}$$

The maximum photon density Q_m is related to the total pulse energy by

$$W=\int_0^\infty Q_m\exp(-2r^2/w^2)\,2\pi r dr=\pi w^2Q_m/2\,. \tag{20}$$

The total reflected pulse energy W_r is calculated from (13) to

$$\begin{aligned} W_r&=\left(\frac{2\pi n_{eh}}{\lambda}\right)^2[1-\exp(-\alpha d)]^2\\ &\quad\times\exp(-\alpha d)\int_0^\infty\frac{c_1c_2c_sQ^3\,2\pi r dr}{3\{1+\sigma Q[1-\exp(-\alpha d)]\}^3}\,. \end{aligned} \tag{21}$$

The FWM reflectivity is obtained as

$$\begin{aligned} R_G=\frac{W_r}{W}&=\left(\frac{2\pi n_{eh}}{\sigma\lambda}\right)^2\frac{c_1c_2\exp(-\alpha d)}{3\sigma AQ_m}\\ &\quad\times\left[\ln(1+\sigma AQ_m)+\frac{2}{1+\sigma AQ_m}\right.\\ &\quad\left.-\frac{1}{2(1+\sigma AQ_m)^2}-\frac{3}{2}\right] \end{aligned} \tag{22}$$

with

$$A=1-\exp(-\alpha d)\,. \tag{23}$$

If $\sigma A Q_m \ll 1$, a quadratic dependence of R_G on Q_m is obtained

$$R_G(\sigma A Q_m \ll 1) \approx \left(\frac{2\pi n_{eh}}{3\sigma\lambda}\right)^2 c_1 c_2 \exp(-\alpha d)\,(\sigma A Q_m)^2$$
$$\approx \left(\frac{2\pi n_{eh}}{3\sigma\lambda}\right)^2 \exp(-\alpha d)\,(\sigma A \sqrt{Q_{m1} Q_{m2}})^2 \quad (24)$$

The dependence of R_G on $\sigma A \sqrt{Q_{m1} Q_{m2}}$ is plotted in Fig. 2. A maximum reflectivity of

$$R_{\max,G} = 0.83\, R_{\max} = 0.83 \left(\frac{4\pi n_{eh}}{9\sigma\lambda}\right)^2 c_1 c_2 \exp(-\alpha d) \quad (25)$$

is obtained at

$$Q_m \approx \sqrt{Q_{m1} Q_{m2}}$$
$$\approx 4.5/\sigma A = \frac{4.5}{\sigma[1-\exp(-\alpha d)]} \approx 2.2\, Q_{\max}\,. \quad (26)$$

In Fig. 2 the dependences of R on $\sigma Q A$, and $R_G(\sigma A \sqrt{Q_{m1} Q_{m2}} \ll 1)$ on $\sigma A \sqrt{Q_{m1} Q_{m2}}$ are also given.

3. Experimental Results

3.1. DFWM *Reflectivity*

The measured reflectivity of DFWM as a function of the mean pump energy density $\sqrt{E_{p1} E_{p2}}$ is shown in Figs. 3 and 4 for sample thickness of 400 and 250 μm, respectively. The solid lines show the theoretical curves, calculated from (22) for different free-carrier absorptions σ and $\alpha = 10\ \mathrm{cm}^{-1}$, $|n_{eh}| = 9 \times 10^{-22}\ \mathrm{cm}^3$ [9, 10].

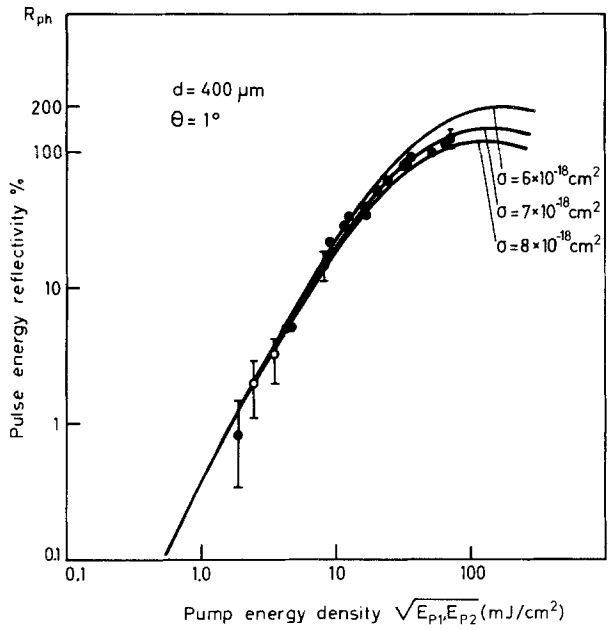

Fig. 3. Dependence of the DFWM reflectivity of silicon with thickness $d = 400$ μm on the average pump energy density

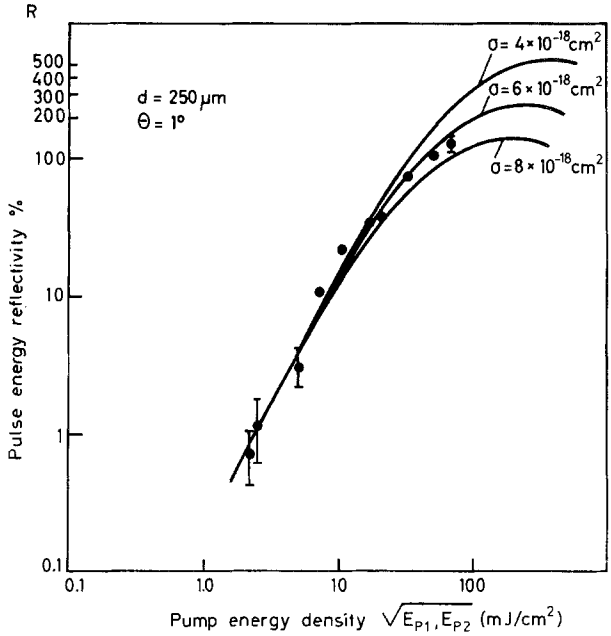

Fig. 4. Dependence of the DFWM reflectivity of silicon with thickness $d = 250$ μm on the average pump energy density

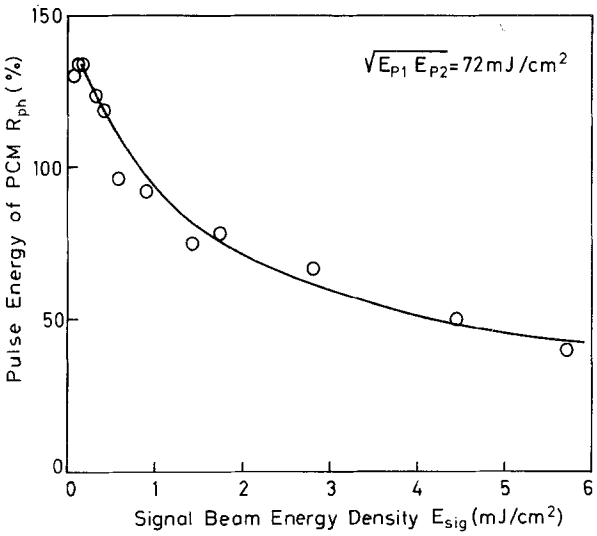

Fig. 5. Dependence of the DFWM reflectivity of silicon on the signal beam energy density

Best agreement between theory and experiment is obtained for $\sigma = (7 \pm 1)\ 10^{-18}\ \mathrm{cm}^2$. This value is larger than the experimental value of Svantesson [9], who obtained from direct absorption measurements $5 \times 10^{-18}\ \mathrm{cm}^2$. The reason may be that also other saturation mechanisms besides free-carrier absorption are present in our experiment, e.g. thermal index changes. Also Svantesson pointed out that spatial fluctuations of the laser-energy density lead to a larger effective absorption coefficient. In addition, laser-induced defocussing of the silicon sample may result in a reduced measured reflectivity.

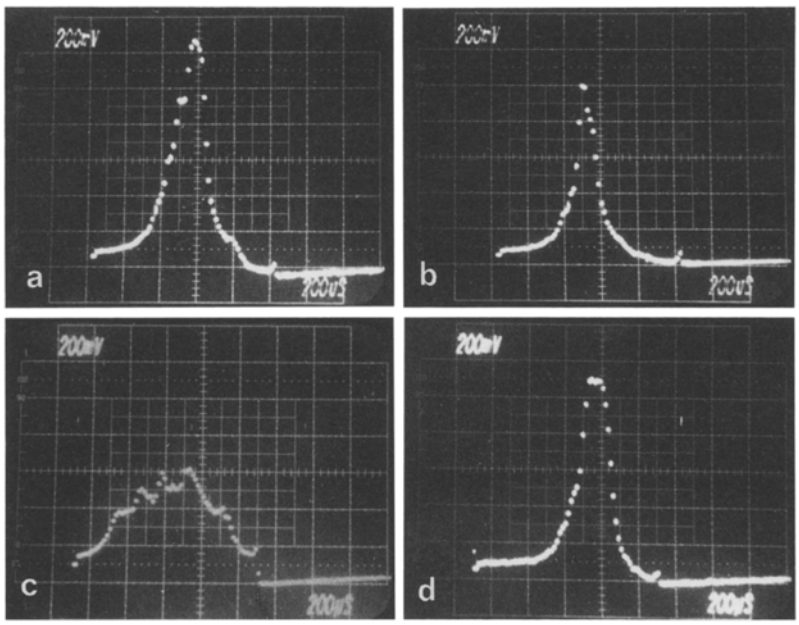

Fig. 6a–d. The profile of a beam reflected by (a) a normal mirror, no lens in the signal beam, (b) a FWM phase conjugate mirror, no lens in the signal beam, (c) a normal mirror with a lens in the signal beam, and (d) a phase conjugate mirror with a lens in the signal beam

A maximum reflectivity of 160% is expected at $\sqrt{E_{p1}E_{p2}} = 155\ \mathrm{mJ/cm^2}$ from the calculations (25). The optimum measured DFWM reflectivity for a 400 μm silicon sample amounts to 125% for $\sqrt{E_{p1}E_{p2}} \approx 70\ \mathrm{mJ/cm^2}$. In this case self-defocusing was remarkable due to the large nonlinear index change [11], [12].

In addition, we have observed that the reflectivity R_{ph} depends on the signal beam energy density E_{sig}. Figure 5 shows as an example the dependence of R_{ph} and E_{sig} for $\sqrt{E_{p1}E_{p2}} = 72\ \mathrm{mJ/cm^2}$.

3.2. Demonstration of the Elimination of Phase Aberration Through the Phase Conjugate Mirror

Since the reflected wave from PCM is time reversed to the signal wave, a spatial phase aberration in the signal beam can be corrected after retraversing the disturbing medium. We used a converging lens in the signal beam as a phase aberrator. The back-focal point of the lens is located behind the sample. If we place a conventional mirror at the position of the PCM, the reflected beam propagates through the lens again and diverges (Fig. 6c). If the PCM is used, the phase-conjugate wave has almost the initial shape after passing the lens again (Fig. 6d).

For comparison, the initial beam profile is shown in Fig. 6a, which was reflected from a normal mirror with no lens in the signal beam. Figure 6b shows the beam profile, which was reflected from the phase conjugate mirror, with no lens in the signal beam. The spatial energy distribution of the various reflected beams was detected with a Spiricon Beam Profiler 2000.

4. Conclusion

The phase-conjugation reflectivity in silicon is limited by free-carrier absorption at high pump energy densities. In this regime strong beam defocussing occurs as will be reported in a following paper. The DFWM reflectivity depends on the signal energy density, so that reflectivities larger than 100% are obtained only at low signal energy densities.

Acknowledgements. This work was supported by the „Deutsche Forschungsgemeinschaft". We thank the IBM Company, Wacker-Chemie-GmbH and Dr. Seifert, Institut für Werkstoffe der Elektrotechnik, TU Berlin, for the silicon samples, Mr. Gerloff for polishing and Mr. Molt for coating.

References

1. J.P. Woerdman, B. Bolger: Phys. Lett. **30**A, 164 (1969)
2. J.P. Woerdman: Opt. Commun. **2**, 212 (1970)
3. K. Jarasiunas, J. Vaitkus: Phys. Status Solidi A **44**, 793 (1977)
4. R.K. Jain, M.B. Klein: Appl. Phys. Lett. **35**, 454 (1979)
5. R.K. Jain, M.B. Klein, R.C. Lind: Opt. Lett. **4**, 328 (1979)
6. R.K. Jain, M.B. Klein: "DFWM in Semiconductors" in *Optical Phase Conjugation*, ed. by R.A. Fischer (Academic, New York 1982)
7. H.J. Eichler, F. Massmann: *Festkörperprobleme* **18** (Vieweg, Braunschweig 1978) pp. 241–263
8. H.J. Eichler, F. Massmann: J. Appl. Phys. **53**, 3237 (1982)
9. K.G. Svantesson: J. Phys. D **12**, 425 (1979)
10. J.P. Woerdman: Phillips Res. Rep. (Suppl.) **7**, 11 (1971)
11. R.K. Jain: Opt. Eng. **21**, 199 (1982)
12. E.W. Van Stryland et al.: In *Picosecond Phenomena* III, ed. by K.B. Eisenthal, R.M. Hochstrasser, W. Kaiser, A. Lambeream, Springer Ser. Chem. Phys. **23** (Springer, Berlin, Heidelberg 1982) p. 368